Inorganic Chemistry

Article

pubs.acs.org/IC

Monometallic Osmium(II) Complexes with Bis(*N*-methylbenzimidazolyl)benzene or -pyridine: A Comparison Study with Ruthenium(II) Analogues

Jiang-Yang Shao[†,‡] and Yu-Wu Zhong*[,†,§]

[†]Beijing National Laboratory for Molecular Sciences, CAS Key Laboratory of Photochemistry, Institute of Chemistry, Chinese Academy of Sciences, Beijing 100190, China

[‡]University of Chinese Academy of Sciences, Beijing 100049, China

[§]State Key Laboratory of Coordination Chemistry, Nanjing University, Nanjing 210093, China

Supporting Information

ABSTRACT: Seven bis-tridentate osmium complexes with Mebib or Mebip (Mebib is the 2-deprotonated form of 1,3-bis(*N*-methylbenzimidazolyl)benzene and Mebip is bis(*N*-methylbenzimidazolyl)pyridine) have been prepared, and their electrochemical and spectroscopic properties are compared with ruthenium structural analogues. Among them, four complexes have the [Os(NCN)(NNN)]-type coordination, including [Os(Mebib)(Mebip)]$(PF_6)_2$ (**1**$(PF_6)_2$), [Os(dpb)(Mebip)](PF_6) (**2**(PF_6), dpb is the 2-deprotonated form of 1,3-di(pyrid-2-yl)benzene), [Os(Mebib)(ttpy)](PF_6) (**3**(PF_6), ttpy = 4′-tolyl-2,2′:6′,2″-terpyridine), and [Os(dpb)(ttpy)](PF_6) (**4**(PF_6)). The other three complexes are [Os(Mebip)$_2$]$(PF_6)_2$ (**5**$(PF_6)_2$), [Os(Mebip)(tpy)]$(PF_6)_2$ (**6**$(PF_6)_2$, tpy = 2,2′:6′,2″-terpyridine), and [Os(ttpy)$_2$]$(PF_6)_2$ (**7**$(PF_6)_2$) with the [Os(NNN)(NNN)]-type coordination. Single crystals of **2**(PF_6) and **6**$(PF_6)_2$ have been obtained, and their structures are studied by X-ray crystallographic analysis. The Os(II/III) redox potentials of **1**$(PF_6)_2$ to **7**$(PF_6)_2$ progressively increase from +0.04, +0.23, +0.24, +0.36, +0.56, +0.79 to +0.94 V vs Ag/AgCl, which are 200−300 mV less positive relative to the Ru(II/III) potentials of their ruthenium counterparts. The highest occupied molecular orbital energy levels of $\mathbf{1}^{+}$−$\mathbf{7}^{2+}$ are calculated to vary in a descending order. The ruthenium and osmium complexes have singlet metal-to-ligand charge-transfer (MLCT) transitions of similar energies and band shapes, while the osmium complexes display additional ^{3}MLCT transitions in the lower-energy region. Complexes **6**$(PF_6)_2$ and **7**$(PF_6)_2$ emit weakly at 780 and 740 nm, respectively. Complex **1**$(PF_6)_2$ was synthesized as the oxidized Os(III) salt because of the low Os(II/III) potential. The transformation of $\mathbf{1}^{2+}$ to $\mathbf{1}^{+}$ by chemical reduction or electrolysis led to the emergence of the ^{1}MLCT transitions in the visible region.

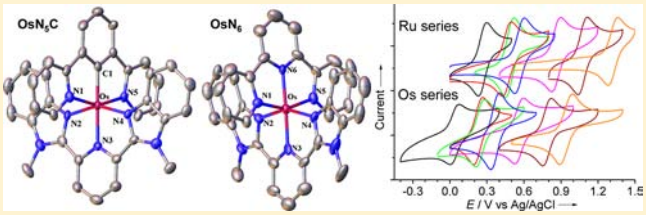

INTRODUCTION

Transition-metal polyazine complexes have attracted enormous attention because of their superior electrochemical and photophysical properties.[1] Among them, cyclometalated complexes are one special type of material that have been the focus of much research efforts.[2] These complexes feature a M−C bond between the metal center and a carbon anionic ligand, for example, the CN-type bidentate ligand or the CNN- or NCN-type tridentate ligand. Transition metals that are mostly involved in cyclometalated complexes include ruthenium,[3] iridium,[4] and platinum.[5] These complexes are very useful in a wide range of applications, such as light-emitting devices,[6] solar cells,[7] and mixed-valence chemistry.[8]

In some applications, the redox potentials of complexes play a crucial role in determining their performance. For instance, low operational potentials would be beneficial for electrochromism (reversible absorption spectral changes in response to external electric field) and would improve the device stability and memory time.[9] In this sense, the use of cyclometalated complexes is very effective. Because of the presence of the anionic cyclometalating ligand, the metal center of cyclometalated complexes is much more electron-rich with respect to the noncyclometalated analogues, and the metal-associated redox potentials are significantly decreased.

Recently, we have reported on a series of cyclometalated ruthenium complexes with the 2-deprotonated form of 1,3-bis(*N*-methylbenzimidazolyl)benzene (MebibH) and bis(*N*-methylbenzimidazolyl)pyridine (Mebip).[10] These complexes display low Ru(II/III) potentials as a result of the electron-donating nature of the carbon anionic ligand and the benzimidazole units. For instance, the Ru(II/III) process of complex [Ru(Mebib)(Mebip)](PF_6) takes places at +0.26 V vs Ag/AgCl, which is considerably lower with respect to the cyclometalated complex [Ru(dpb)(tpy)](PF_6) ($E_{1/2}$ = 0.56 V) and the noncyclometalated complex [Ru(tpy)$_2$]$(PF_6)_2$ ($E_{1/2}$ = 1.32 V), where dpb is the 2-deprotonated form of 1,3-di(pyrid-2-yl)benzene (dpbH) and tpy is 2,2′:6′,2″-terpyridine. As an

Received: February 13, 2013
Published: May 21, 2013

   dx.doi.org/10.1021/ic400385b | *Inorg. Chem.* 2013, 52, 6464−6472

Scheme 1. Syntheses of Compounds Studied

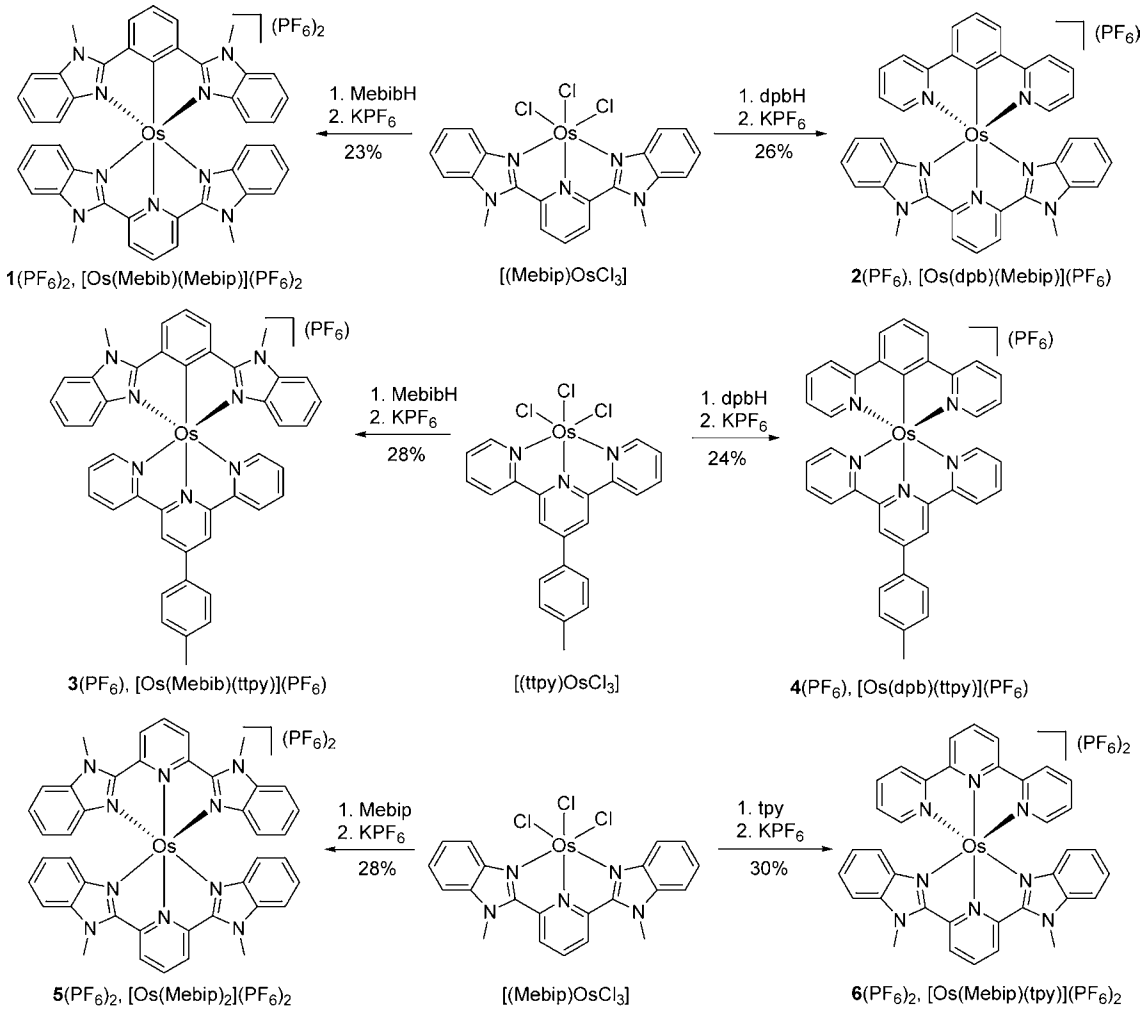

extension of this work, we considered that the use of osmium would be possible to further decrease the metal-based redox potentials. Osmium polyazine complexes have been well-known to possess well-defined Os(II/III) processes with much lower redox potentials relative to ruthenium structural analogues.[11]

Compared to cyclometalated ruthenium complexes, only limited reports have been devoted to the syntheses and studies of cyclometalated osmium complexes.[12] Le Lagadec and Ryabov and co-workers have synthesized a series of cyclometalated osmium complexes with a general formula of $[Os(C-N)_x(N-N)_{3-x}]^{m+}$ (x = 0−3),[13] where C−N is a bidentate cyclometalating ligand and N−N is a bidentate ligand, such as 2,2′-bipyridine and 1,10-phenanthroline. These complexes have low redox potentials and high rates of oxidation of reduced enzymes. Collin and Barigelletti and co-workers reported a few [Os(NCN)(NNN)]-type bis-tridentate polypyridyl osmium complexes and related dimetallic complexes bridged by a biscyclometalating ligand.[14] Recently, some emissive osmium complexes supported by N-heterocyclic carbene-based CCC-pincer ligands and aromatic diimines have been disclosed by Wong and co-workers.[15] We note that, although a large number of transition-metal complexes with Mebip or Mebib have been known,[16] osmium complexes with these two ligands, either cyclometalated or noncyclometalated, have not been documented to date. We present in this Article the syntheses and characterization of a series of osmium complexes with Mebip or Mebib (Scheme 1) and a comparison study of their electrochemical and spectroscopic properties with the previously reported ruthenium analogues.[10a] In addition, theoretical calculations have been performed to complement these experimental results.

RESULTS AND DISCUSSION

Syntheses and X-ray Structures. The osmium complexes studied in the paper were synthesized as outlined in Scheme 1. The reaction of $(NH_4)_2[OsCl_6]$ with Mebip afforded $[(Mebip)OsCl_3]$ in good yield. The treatment of $[(Mebip)OsCl_3]$ with MebibH in ethylene glycol under microwave heating, followed by anion exchange using KPF_6, gave complex $[Os(Mebib)(Mebip)](PF_6)_2$ ($\mathbf{1}(PF_6)_2$) in 23% yield. This reaction was expected to give a cyclometalated Os(II) complex with one anion. However, only the oxidized Os(III) form was isolated, suggesting that the Os(II/III) potential is sufficiently low. The identity of $\mathbf{1}(PF_6)_2$ was supported by mass spectrum, microanalysis, and following spectroelectrochemical measurement. Using a similar procedure, the reaction of $[(Mebip)OsCl_3]$ with dpbH, Mebip, and tpy gave the cyclometalated complex $[Os(dpb)(Mebip)](PF_6)$ ($\mathbf{2}(PF_6)$) and noncyclometalated complexes $[Os(Mebip)_2](PF_6)_2$ ($\mathbf{5}(PF_6)_2$) and $[Os(Mebip)(tpy)](PF_6)_2$ ($\mathbf{6}(PF_6)_2$), respectively. Cyclometalated complexes $[Os(Mebib)(ttpy)](PF_6)$ ($\mathbf{3}(PF_6)$, ttpy = 4′-tolyl-2,2′:6′,2″-terpyridine)[17] and $[Os(dpb)(ttpy)](PF_6)$ ($\mathbf{4}(PF_6)$)

dx.doi.org/10.1021/ic400385b | Inorg. Chem. 2013, 52, 6464−6472

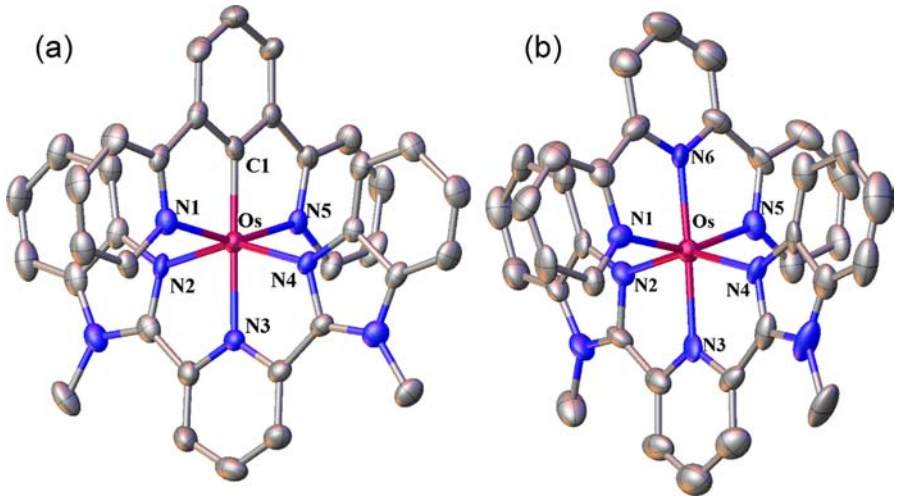

Figure 1. Thermal ellipsoid plots of the X-ray structures of (a) $\mathbf{2}(PF_6)$ and (b) $\mathbf{6}(PF_6)_2$ with 30% probability. Counter anions and hydrogen atoms are omitted for clarity. Atom color code: carbon, gray; nitrogen, blue; osmium, brown.

were prepared from the reaction of $[(ttpy)OsCl_3]$[14] with MebibH and dpbH, respectively. The yields for the syntheses of these complexes are in the range of 20−30%. Some byproducts with higher polarity were detected in thin-layer chromatography. However, their composition has not been identified. The addition of AgOTf in these reactions, as has been used in the syntheses of ruthenium analogues,[10] did not improve the yield. In addition to these complexes, a known compound $[Os(ttpy)_2](PF_6)_2$ ($\mathbf{7}(PF_6)_2$) was prepared for a comparison study.[18]

Single crystals of $\mathbf{2}(PF_6)$ and $\mathbf{6}(PF_6)_2$ suitable for X-ray analysis were obtained by diffusion of diethyl ether into the solution of these two compounds in CH_3CN. The thermal ellipsoid plots of the X-ray structures are shown in Figure 1. Crystal data and selected bond lengths and angles are given in Tables 1 and 2. The bis-tridentate coordination mode is confirmed for both complexes. In complex $\mathbf{2}(PF_6)$, the Mebib ligand binds to osmium with an NCN-type coordination. The Os−C1 bond length is 1.977(8) Å. The Os−N bonds are in the range of 2.058(4)−2.087(7) Å. In complex $\mathbf{6}(PF_6)_2$, the bond between osmium and the central pyridine nitrogen (N6) of tpy is the shortest Os−N bond in length. The Os−N3 bond, opposite to Os−N6, has a length of 2.023(6) Å. Other Os−N bonds are in the range of 2.060(6)−2.072(6) Å.

Table 1. Crystallographic Data

compound	$\mathbf{2}(PF_6)$	$\mathbf{6}(PF_6)_2$
empirical formula	$C_{37}H_{28}N_7OsPF_6$	$C_{36}H_{28}N_8OsP_2F_{12}$
formula weight	905.83	1052.81
space group	$P\bar{1}$	$P\bar{1}$
crystal system	triclinic	triclinic
a (Å)	9.257(2)	13.1990(18)
b (Å)	11.733(3)	18.001(3)
c (Å)	17.132(5)	18.683(2)
α (deg)	97.50	95.03
β (deg)	99.13	90.19
γ (deg)	111.02	104.01
vol (Å^3)	1679.1(7)	4289.0(10)
Z	2	2
R_1 (all)	0.0531	0.0749
R_1 (gt)	0.0458	0.0594
wR_2 (ref)	0.1529	0.1853
wR_2 (gt)	0.1249	0.1734

Electrochemical Studies. Figure 2 shows the cyclic voltammograms (CVs) of the above synthesized osmium complexes. The electrochemical data are summarized in Table 3, together with those of the previously reported ruthenium analogues.[10a] Cyclometalated complexes $\mathbf{1}(PF_6)_2$ to $\mathbf{4}(PF_6)$ show one cathodic wave at −1.63, −1.57, −1.53, and −1.48 V vs Ag/AgCl, respectively. They are assigned to the reduction of the individual noncyclometalating (NNN) ligand, Mebip of $\mathbf{1}(PF_6)_2$ and $\mathbf{2}(PF_6)$, and ttpy of $\mathbf{3}(PF_6)$ and $\mathbf{4}(PF_6)$, respectively. The anionic cyclometalating (NCN) ligand is more electron-rich and thus sluggish to be reduced relative to the NNN ligand. Within the solvent window, complexes $\mathbf{1}(PF_6)_2$ to $\mathbf{4}(PF_6)$ all display two peaks in the anodic scan. The less positive redox couples at +0.04, +0.23, +0.24, and +0.36 V vs Ag/AgCl for $\mathbf{1}(PF_6)_2$ to $\mathbf{4}(PF_6)$, respectively, are attributed to the Os(II/III) processes. It is possible that some mixing of ligand oxidation is involved in this process, a common feature for cyclometalated complexes.[3] It is not surprising that complex $\mathbf{1}(PF_6)_2$ was isolated in the oxidized form because of its low Os(II/III) potential. The more positive redox waves of $\mathbf{1}(PF_6)_2$ to $\mathbf{4}(PF_6)$ (mostly irreversible except $\mathbf{1}(PF_6)_2$) are ascribed to the Os(III/IV) processes.

Noncyclometalated complexes $\mathbf{5}(PF_6)_2$ to $\mathbf{7}(PF_6)_2$ all show two ligand-based reduction waves. The Os(II/III) process occurs at +0.56, +0.79, and +0.94 V vs Ag/AgCl for $\mathbf{5}(PF_6)_2$, $\mathbf{6}(PF_6)_2$, and $\mathbf{7}(PF_6)_2$, respectively. The Os(II/III) potentials for noncyclometalated complexes are clearly more positive with respect to cyclometalated complexes $\mathbf{1}(PF_6)_2$ to $\mathbf{4}(PF_6)$. The Os(II/III) potentials of osmium complexes $\mathbf{1}(PF_6)_2$ to $\mathbf{7}(PF_6)_2$, either cyclometalated or not, are 200−300 mV less positive relative to the Ru(II/III) potentials of their ruthenium counterparts (Table 3). This is caused by the lower third ionization energy for Os relative to Ru.[11]

Density Functional Theory (DFT) Calculations. DFT calculations were performed for $\mathbf{1}^+$−$\mathbf{7}^{2+}$ on the B3LYP/LANL2DZ/6-31G*/CPCM level of theory (see details in the Experimental Section). Figure 3 shows the calculated energy diagrams of these complexes. The highest occupied molecular orbital (HOMO) levels progressively descend from −4.66 eV for $\mathbf{1}^+$ to −5.88 eV for $\mathbf{7}^{2+}$. This order is in good accordance

dx.doi.org/10.1021/ic400385b | Inorg. Chem. 2013, 52, 6464−6472

Table 2. Selected Bond Lengths and Bond Angles

bond lengths (Å)		bond angles (deg)	
$2(PF_6)$	$6(PF_6)_2$	$2(PF_6)$	$6(PF_6)_2$
Os–N(1) 2.074(6)	Os–N(1) 2.070(5)	C(1)–Os–N(1) 77.9(3)	N(6)–Os–N(1) 78.2(2)
Os–N(2) 2.061(5)	Os–N(2) 2.072(6)	C(1)–Os–N(2) 101.8(3)	N(6)–Os–N(2) 104.6(2)
Os–N(3) 2.066(6)	Os–N(3) 2.023(6)	C(1)–Os–N(3) 178.8(3)	N(6)–Os–N(3) 177.5(2)
Os–N(4) 2.058(4)	Os–N(4) 2.065(6)	N(3)–Os–N(1) 102.3(2)	N(3)–Os–N(1) 102.1(2)
Os–N(5) 2.087(7)	Os–N(5) 2.060(6)	N(3)–Os–N(2) 77.0(2)	N(3)–Os–N(2) 77.9(2)
Os–C(1) 1.977(8)	Os–N(6) 1.993(5)		

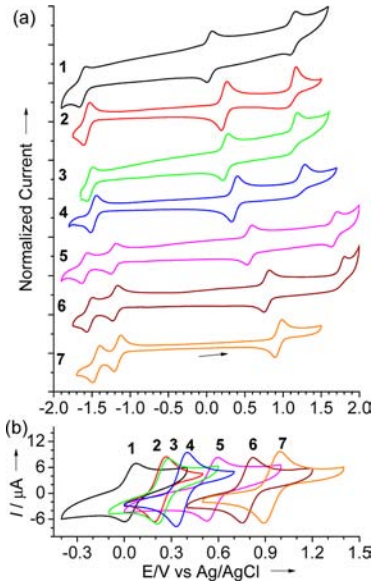

Figure 2. (a) CVs of $1(PF_6)_2$ to $7(PF_6)$ (anions are omitted for complex labels) in 0.1 M Bu_4NClO_4/CH_3CN at 100 mV/s. (b) A comparison of the Os(II/III) waves.

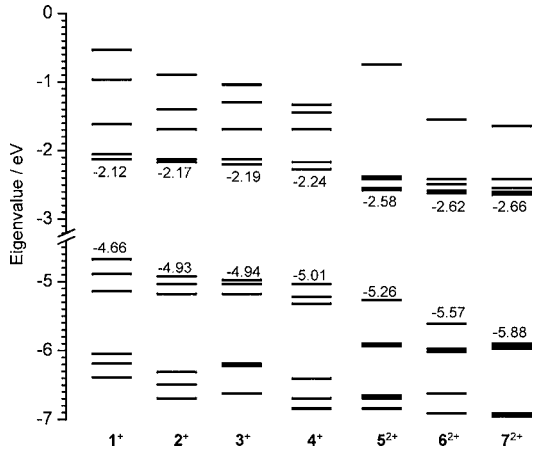

Figure 3. DFT-calculated energy diagrams of 1^+–7^{2+}. The numbers shown in the middle indicate the LUMO and HOMO energies.

with the Os(II/III) potentials of these complexes (Figure 2 and Table 3). The lowest unoccupied molecular orbital (LUMO) levels of these complexes have the same descending order from 1^+ to 7^{2+}, which also correlates well with the first reduction potentials of these complexes.

The closely spaced HOMO, HOMO−1, and HOMO−2 of 1^+ have major contributions from the osmium atom (Figure 4), except that the HOMO−1 has some contributions from the cyclometalating phenyl ring. The much lower-lying HOMO−3, HOMO−4, and HOMO−5 are dominated by the NCN ligand (Mebib) and NNN (Mebip) ligand, respectively. The closely spaced LUMO and LUMO+1 of 1^+ have major contributions from the NNN ligand and a minor contribution from the osmium atom. This feature has not been observed for cyclometalated ruthenium complexes,[10] reflecting the greater extension of osmium d orbitals.[11] However, it should be kept in mind that DFT calculations tend to overestimate electron delocalization. The higher-lying LUMO+2 level is dominated by the NCN ligand. Other three cyclometalated complexes (2^+–4^+) have very similar frontier orbital orderings and

Table 3. Electrochemical and Absorption Data

complex[a]	$E_{1/2}$[b] (anodic)	$E_{1/2}$[b] (cathodic)	λ_{max}/nm ($\varepsilon/10^5$ M^{-1} cm^{-1})[c]
$[Os(Mebib)(Mebip)]^{2+}$, 1^{2+}	+0.04, +1.13	−1.63	354 (0.23), 510 (0.16), 590 (0.057)
$[Ru(Mebib)(Mebip)]^{+}$[d]	+0.26, +1.50	−1.60	334 (0.32), 353 (0.27), 515 (0.13), 571 (0.077)
$[Os(dpb)(Mebip)]^{+}$, 2^+	+0.23, +1.18[e]	−1.57	350 (0.32), 450 (0.13), 510 (0.16), 800 (0.011)
$[Ru(dpb)(Mebip)]^{+}$[d]	+0.43, +1.49[e]	−1.56	334 (0.29), 339 (0.39), 457 (0.12), 516 (0.17)
$[Os(Mebib)(ttpy)]^{+}$, 3^+	+0.24, +1.17[e]	−1.53	396 (0.17), 470 (0.19), 514(0.18), 864 (0.021)
$[Ru(Mebib)(tpy)]^{+}$[d]	+0.48, +1.47	−1.55	275 (0.47), 319 (0.44), 394 (0.082), 497 (0.11)
$[Os(dpb)(ttpy)]^{+}$, 4^+	+0.36, +1.27[e]	−1.48	372 (0.20), 502 (0.20), 538 (0.19), 764 (0.025)
$[Ru(dpb)(tpy)]^{+}$[d,f]	+0.56, +1.60[e]	−1.51	372 (0.086), 423 (0.095), 499 (0.14)
$[Os(Mebip)_2]^{2+}$, 5^{2+}	+0.56, +1.67	−1.22, −1.60	360 (0.71), 486 (0.20), 564 (0.071), 798 (0.018)
$[Ru(Mebip)_2]^{2+}$[d]	+0.86	−1.24, −1.55	357 (0.66), 491 (0.16)
$[Os(Mebip)(tpy)]^{2+}$, 6^{2+}	+0.79, +1.81[e]	−1.20, −1.53	356 (0.39), 480 (0.15), 542 (0.063), 718 (0.028)
$[Ru(Mebip)(tpy)]^{2+}$[d]	+1.07	−1.24, −1.50	354 (0.38), 480 (0.14)
$[Os(ttpy)_2]^{2+}$, 7^{2+}	+0.94	−1.17, −1.45	314 (0.72), 490 (0.25), 668 (0.064)
$[Ru(tpy)_2]^{2+}$[d,f]	+1.32	−1.22, −1.46	307 (0.78), 475 (0.17)

[a]All anions are PF_6^-. [b]The potential is reported as the $E_{1/2}$ value vs Ag/AgCl. The potential value vs ferrocene$^{0/+}$ can be deduced by subtracting 0.45 V. [c]All absorption spectra were recorded in CH_3CN at room temperature. [d]See ref 10a. [e]$E_{p,anodic}$, irreversible. [f]See ref 3i.

dx.doi.org/10.1021/ic400385b | Inorg. Chem. 2013, 52, 6464−6472

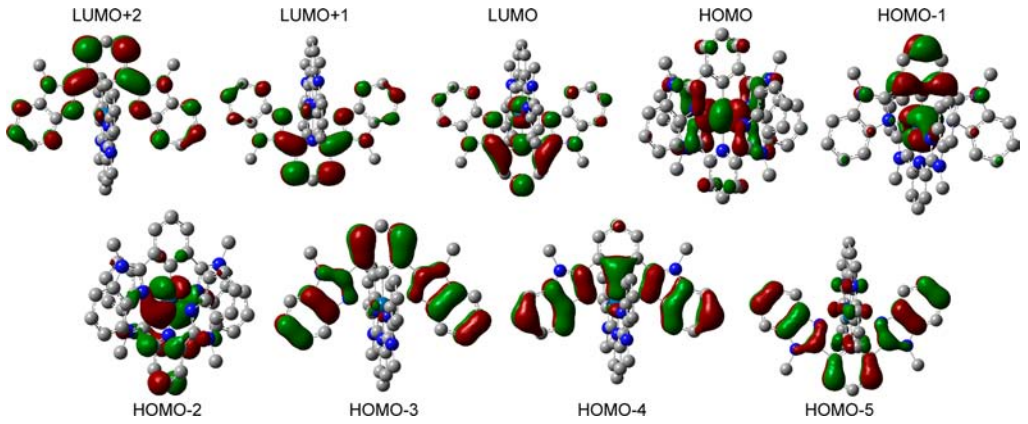

Figure 4. Selected frontier orbital graphics of $\mathbf{1}^+$. The upper and lower parts of the structure are Mebib and Mebip, respectively.

compositions as $\mathbf{1}^+$ (Figures S1−S3 in the Supporting Information), except that the HOMOs, instead of HOMO−1, of $\mathbf{2}^+$−$\mathbf{4}^+$ have some contributions from the cyclometalating phenyl ring. These calculation results support the previous electrochemical assignment that the observed cathodic waves of $\mathbf{1}^{2+}$−$\mathbf{4}^+$ are associated with their NNN ligands, and the first anodic waves are the $Os^{II/III}$ processes, possibly mixing with some portion of ligand oxidation.

Selected frontier orbitals with electron density distributions of the noncyclometalated complexes $\mathbf{5}^{2+}$−$\mathbf{7}^{2+}$ are provided in Figures S4−S6 (Supporting Information). Complexes $\mathbf{5}^{2+}$ and $\mathbf{7}^{2+}$ have symmetrical structures, and their occupied and unoccupied frontier orbitals are dominated by osmium and individual ligands, respectively. For the asymmetric complex $\mathbf{6}^{2+}$, the LUMO and LUMO+1 are dominated by Mebip and tpy ligands, respectively (Figure S5, Supporting Information).

Spectroscopic Studies and Time-Dependent DFT (TDDFT) Calculations. The UV/vis absorption spectra of $\mathbf{1}^+$ to $\mathbf{7}(PF_6)_2$ ($\mathbf{1}^+$ was obtained by chemical reduction; see below) are displayed in Figure 5, and the absorption data are summarized in Table 3. Complexes $\mathbf{1}^+$, $\mathbf{2}(PF_6)$, $\mathbf{5}(PF_6)_2$, and $\mathbf{6}(PF_6)_2$ show intense Mebip-based intraligand (IL) transitions around 350 nm. Other IL transitions locate at a slightly higher-energy region. This feature has previously been observed for the ruthenium complexes with Mebip.[10a] Absorption bands in the visible region are due to the singlet metal-to-ligand charge-transfer (^{1}MLCT) transitions. Most complexes, especially $\mathbf{3}(PF_6)$ to $\mathbf{7}(PF_6)_2$, show distinct shallow absorption in the region of 650−900 nm. These are ascribed to the spin-forbidden ^{3}MLCT transitions, a well-known feature for polyazine osmium complexes caused by the strong spin−orbital coupling of osmium.[11−14] The solvent dependence of the absorption spectra of both cyclometalated and noncyclometalated complexes, represented by $\mathbf{2}(PF_6)$ and $\mathbf{6}(PF_6)_2$, are insignificant (Figures S7 and S8, Supporting Information).

The ^{1}MLCT transitions of cyclometalated complexes are much more broad and complex with respect to those of noncyclometalated complexes. To assist the understanding of these transitions, TDDFT calculations have been performed for the singlet states of asymmetric complexes $\mathbf{1}^+$, $\mathbf{2}^+$, $\mathbf{3}^+$, $\mathbf{4}^+$, and $\mathbf{6}^{2+}$ (Figure 6, and Table S1 in the Supporting Information). These results suggest that the MLCT bands of $\mathbf{1}^+$−$\mathbf{4}^+$ are all associated with both NCN and NNN ligands. For example, the calculated S_5 and S_6 excitations of $\mathbf{1}^+$ are responsible for the observed shoulder band around 520 nm and S_7 and S_8 excitations are responsible for the MLCT band with the

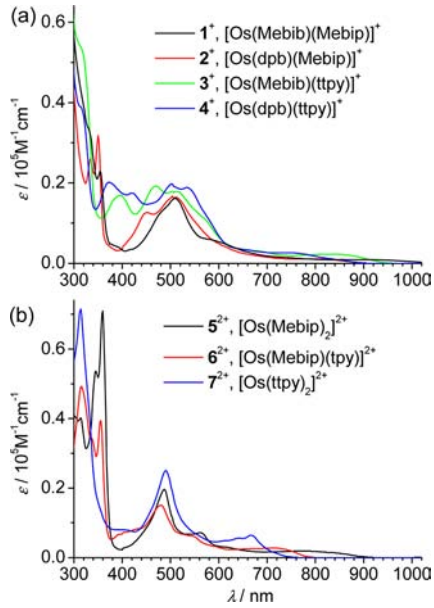

Figure 5. UV/vis absorption spectra of (a) cyclometalated complexes $\mathbf{1}^+$ to $\mathbf{4}(PF_6)$ and (b) noncyclometalated complexes $\mathbf{5}(PF_6)_2$ to $\mathbf{7}(PF_6)_2$ in CH_3CN. Anions are omitted for the complex labels for clarity.

absorption maximum at 440 nm. These four excitations are mainly of the HOMO−2 → LUMO+1, HOMO → LUMO+2, HOMO−1 → LUMO+2, and HOMO−2 → LUMO character, respectively, where LUMO and LUMO+1 have dominant contributions from the NNN ligand and LUMO+2 from the NCN ligand. Symmetrical noncyclometalated complexes $\mathbf{5}(PF_6)_2$ and $\mathbf{7}(PF_6)_2$ display ^{1}MLCT absorption maxima at 486 and 490 nm, respectively. For the asymmetric complex $\mathbf{6}^2$+, TDDFT results suggest that the ^{1}MLCT transitions are associated both Mebip and ttpy ligands.

Figure S9 in the Supporting Information provides a comparison of the absorption spectra of the Os series complexes with their ruthenium counterparts (Ru series). Two series compounds have similar ^{1}MLCT absorption shapes and energies, but no ^{3}MLCT transitions are observed for the Ru series compounds. Complexes $\mathbf{3}(PF_6)$, $\mathbf{4}(PF_6)$, and $\mathbf{7}(PF_6)_2$ have a slightly higher ^{1}MLCT molar absorptivity relative to their ruthenium counterparts, $[Ru(Mebib)(tpy)](PF_6)$, $[Ru(dpb)(tpy)](PF_6)$, and $[Ru(tpy)_2](PF_6)_2$, respectively. This is partially caused by the use of one different auxiliary ligand, tpy

dx.doi.org/10.1021/ic400385b | Inorg. Chem. 2013, 52, 6464−6472

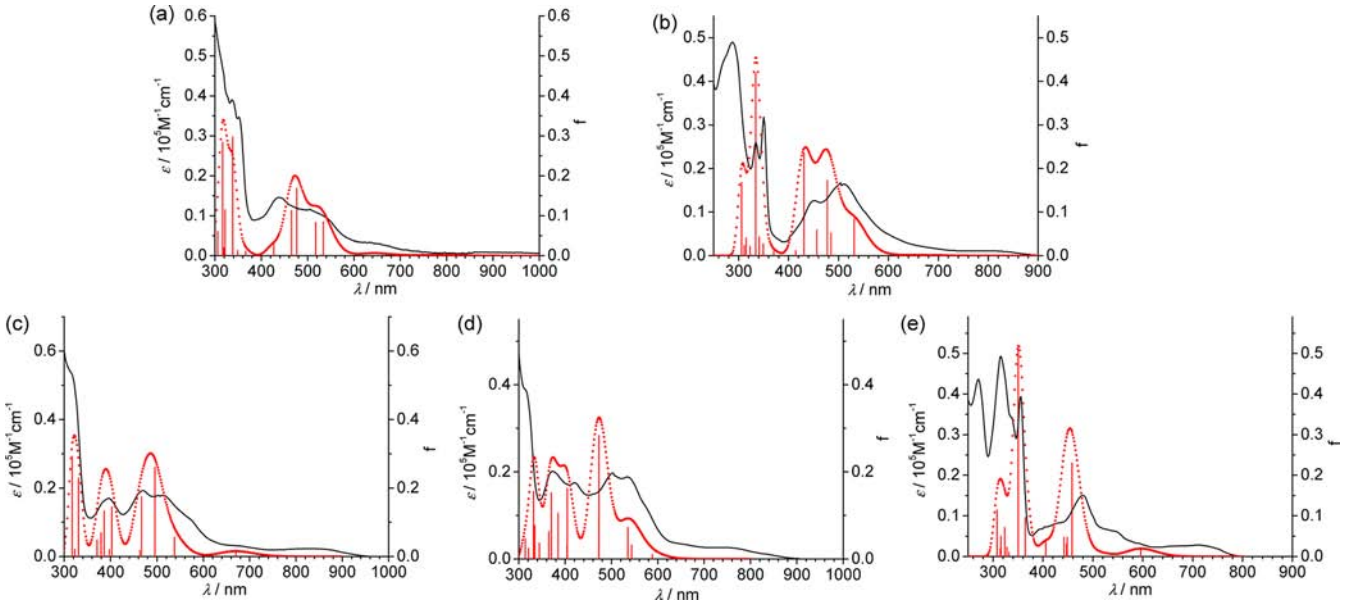

Figure 6. UV/vis absorption spectra (black curves) and TDDFT-predicted singlet excitations (vertical lines and red dotted curves) of (a) $\mathbf{1}^{+}$, (b) $\mathbf{2}^{+}$, (c) $\mathbf{3}^{+}$, (d) $\mathbf{4}^{+}$, and (e) $\mathbf{6}^{2+}$. The left and right *y* axes are associated with the absorption spectra and predicted excitations, respectively.

for the Ru series and ttpy for the Os ttpy series. Complex $\mathbf{7}(PF_6)_2$ was previously reported to show an emission band around 750 nm at room temperature.[18a] Similarly, we have recorded a weak emission at 740 nm for this complex (Figure 7). In addition, the asymmetric noncyclometalated complex $\mathbf{6}(PF_6)_2$ was found to emit weakly at 780 nm. However, no distinct emission was detected for other complexes.

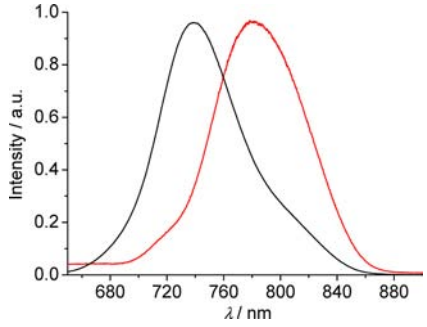

Figure 7. Emission spectra of $\mathbf{6}(PF_6)_2$ (red line) and $\mathbf{7}(PF_6)_2$ (black line) in CH_3CN at room temperature. The excitation wavelength is 480 nm.

As has been mentioned earlier, $\mathbf{1}(PF_6)_2$ was isolated as the Os(III) form. When $\mathbf{1}(PF_6)_2$ was treated with aqueous hydrazine ($NH_2NH_2{\cdot}H_2O$) in CH_3CN,[19] the absorption band at 420 nm decreased and the ^{1}MLCT transition at 510 nm, associated with the reduced form $\mathbf{1}^{+}$, was recovered (Figure 8). The appearance of isosbestic absorption points at 338 and 460 nm indicates the clean transformation of this process. The reduction of $\mathbf{1}(PF_6)_2$ can also be triggered by electrolysis with an indium tin oxide (ITO) glass electrode by gradually decreasing the potential from the open-circuit potential to −0.6 V vs Ag/AgCl (Figure S10, Supporting Information).

CONCLUSION

In summary, we have successfully prepared a series of cyclometalated and noncyclometalated osmium complexes

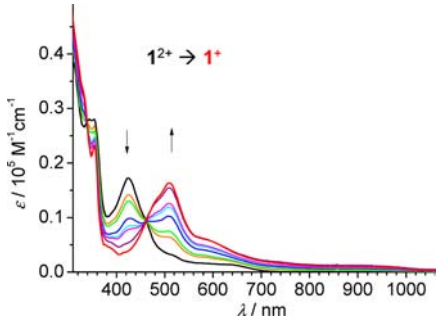

Figure 8. Absorption spectral changes of $\mathbf{1}(PF_6)_2$ in CH_3CN during stepwise reduction with $NH_2NH_2{\cdot}H_2O$.

containing the Mebib or Mebip ligands. The Os(II/III) potentials of these complexes can be modulated in a wide range from +0.04 to +0.94 V vs Ag/AgCl, which are 200−300 mV less positive relative to the Ru(II/III) potentials of their ruthenium counterparts. This feature may make osmium complexes applicable for redox-controlled processes, such as mixed-valence chemistry,[8,10b] electrochromism,[9] and electrocatalysis.[13] The newly prepared osmium complexes show absorption in the near-infrared (NIR) region due to the ^{3}MLCT transitions, and they can be considered as potential dyes for solar cell applications. In this sense, the cyclometalated complexes are of little interest, because their HOMO levels are too high for dye regeneration.[7] It would be better to design dye compounds on the basis of the noncyclometalated complexes with lower-lying HOMO levels.

EXPERIMENTAL SECTION

General Procedure. NMR spectra were recorded in designated solvents on a Bruker Avance 400 MHz spectrometer. Spectra are reported in parts per million values from residual protons of deuterated solvents. Mass spectra (MS) data were obtained with a Bruker Daltonics Inc. ApexII FT-ICR or Autoflex III MALDI-TOF mass spectrometer. The matrix is α-cyano-4-hydroxycinnamic acid. Microanalysis was carried out using a Flash EA 1112 analyzer at the Institute of Chemistry, Chinese Academy of Sciences. Mebip,[10a]

dx.doi.org/10.1021/ic400385b | Inorg. Chem. 2013, 52, 6464−6472

MebibH,[10a] ttpy,[17] dpbH,[20] and $[Os(ttpy)_2](PF_6)_2$[18] were prepared according to known procedures.

Synthesis of [Os(Mebip)Cl$_3$]. To 10 mL of dry *N*,*N*-dimethyl formamide were added $(NH_4)_2[OsCl_6]$ (207.8 mg, 0.47 mmol) and Mebip (176.1 mg, 0.52 mmol). The mixture was refluxed for 1 h. After cooling to room temperature, the mixture was poured into 30 mL of ethyl ether. The resulting precipitate was collected by filtering and washing with ethyl ether to give 214 mg of $[Os(Mebip)Cl_3]$ as a black solid in 70% yield. MALDI-MS: 601.0 for $[M - Cl]^+$.

Synthesis of [Os(ttpy)Cl$_3$]. To 10 mL of dry *N*,*N*-dimethyl formamide were added $(NH_4)_2[OsCl_6]$ (219 mg, 0.50 mmol) and ttpy (161 mg, 0.52 mmol). The mixture was refluxed for 1 h. After cooling to room temperature, the mixture was poured into 30 mL of ethyl ether. The resulting precipitate was collected by filtering and washing with ethyl ether to give 252 mg of $[Os(ttpy)Cl_3]$ as a black solid in 81% yield. MALDI-MS: 584.9 for $[M - Cl]^+$.

Synthesis of Complex [Os(Mebib)(Mebip)](PF$_6$)$_2$, 1(PF$_6$)$_2$. To 10 mL of dry ethylene glycol were added $[(Mebip)OsCl_3]$ (34.5 mg, 0.054 mmol) and MebibH (16.9 mg, 0.050 mmol). The mixture was refluxed for 0.5 h under microwave heating (power = 375 W). After cooling to room temperature, an excess of aq. KPF_6 was added. The resulting precipitate was collected by filtrating and washing with water and Et_2O. The obtained solid was subjected to flash column chromatography on silica gel (eluent: CH_3CN/H_2O/aq. KNO_3, 100/5/0.5), followed by anion exchange with KPF_6, to give 11.4 mg of $\mathbf{1}(PF_6)_2$ in 23% yield as a black solid. MALDI-MS: 868.5 for $[M - 2PF_6]^+$. Anal. Calcd for $C_{43}H_{34}F_{12}N_9P_2Os{\cdot}H_2O$: C, 43.96; H, 3.09; N, 10.73. Found: C, 43.84; H, 3.28; N, 10.72.

Synthesis of Complex [Os(Mebip)(dpb)](PF$_6$), 2(PF$_6$). Using the same procedure for the synthesis of $\mathbf{1}(PF_6)_2$, 12.2 mg of complex $\mathbf{2}(PF_6)$ was isolated from the reaction of $[(Mebip)OsCl_3]$ (32.5 mg, 0.051 mmol) with dpbH (18.5 mg, 0.080 mmol) in 26% yield. ^{1}H NMR (400 MHz, CD_3CN): δ 4.54 (s, 6H), 5.98 (d, J = 8.0 Hz, 2H), 6.46 (t, J = 6.4 Hz, 2H), 6.75 (t, J = 8.0 Hz, 2H), 6.86 (m, 2H), 7.28 (t, J = 7.4 Hz, 4H), 7.46 (d, J = 8.0 Hz, 4H), 8.04 (d, J = 8.4 Hz, 2H), 8.43 (d, J = 7.6 Hz, 2H), 8.54 (m, 2H). MALDI-MS: 762.4 for $[M - PF_6]^+$. Anal. Calcd for $C_{37}H_{28}F_6N_7POs$: C, 49.06; H, 3.12; N, 10.82. Found: C, 49.15; H, 3.09; N, 10.78.

Synthesis of Complex [Os(Mebib)(ttpy)](PF$_6$), 3(PF$_6$). Using the same procedure for the synthesis of $\mathbf{1}(PF_6)_2$, 14.0 mg of $\mathbf{3}(PF_6)$ was isolated from the reaction of $[(ttpy)OsCl_3]$ (32.0 mg, 0.052 mmol) and MebibH (17.0 mg, 0.050 mmol) in 28% yield. ^{1}H NMR (400 MHz, CD_3CN): δ 2.56 (s, 3H), 4.45 (s, 6H), 5.35 (t, J = 7.2 Hz, 1H), 5.58 (s, 2H), 6.70 (t, J = 7.6 Hz, 2H), 6.96–7.06 (m, 4H), 7.24–7.36 (m, 8H), 7.55 (d, J = 8.0 Hz, 2H), 8.14 (d, J = 7.2 Hz, 2H), 8.49 (d, J = 8.0 Hz, 2H), 8.94 (s, 2H). MALDI-MS: 852.6 for $[M - PF_6]^+$. Anal. Calcd for $C_{44}H_{34}F_6N_7POs$: C, 53.06; H, 3.44; N, 9.84. Found: C, 53.29; H, 3.64; N, 10.10.

Synthesis of Complex [Os(ttpy)(dpb)](PF$_6$), 4(PF$_6$).[14] Using the same procedure for the synthesis of $\mathbf{1}(PF_6)_2$, 10.8 mg of $\mathbf{4}(PF_6)$ was isolated from the reaction of $[(ttpy)OsCl_3]$ (31.2 mg, 0.050 mmol) and dpbH (17.0 mg, 0.050 mmol) in 24% yield. ^{1}H NMR (400 MHz, CD_3CN): δ 2.53 (s, 3H), 6.55 (t, J = 6.2 Hz, 2H), 6.86–6.92 (m, 4H), 7.11 (d, J = 4.4 Hz, 2H), 7.30 (s, 1H), 7.46 (t, J = 7.0 Hz, 2H), 7.53 (d, J = 7.6 Hz, 2H), 7.58 (t, J = 7.2 Hz, 2H), 8.06 (d, J = 8.4 Hz, 2H), 8.17 (d, J = 8.0 Hz, 2H), 8.35 (d, J = 7.6 Hz, 2H), 8.57 (d, J = 8.0 Hz, 2H), 8.99 (s, 2H). MALDI-MS: 744.4 for $[M - PF_6]^+$. Anal. Calcd for $C_{38}H_{28}F_6N_5POs{\cdot}3H_2O$: C, 48.35; H, 3.63; N, 7.42. Found: C, 48.43; H, 3.27; N, 7.54.

Synthesis of Complex [Os(Mebip)$_2$](PF$_6$)$_2$, 5(PF$_6$)$_2$. Using the same procedure for the synthesis of $\mathbf{1}(PF_6)_2$, 10.9 mg of $\mathbf{5}(PF_6)_2$ was isolated from the reaction of $[(Mebip)OsCl_3]$ (31.9 mg, 0.050 mmol) and Mebip (17.5 mg, 0.050 mmol) in 19% yield. ^{1}H NMR (400 MHz, CD_3CN): δ 4.52 (s, 12H), 6.17 (d, J = 8.4 Hz, 4H), 6.92 (t, J = 7.6 Hz, 4H), 7.35 (t, J = 7.8 Hz, 4H), 7.42 (d, J = 8.4 Hz, 4H), 7.73 (d, J = 8.4 Hz, 2H), 8.76 (d, J = 8.4 Hz, 4H). MALDI-MS: 1014.5 for $[M - PF_6]^+$, 870.5 for $[M - 2PF_6]^+$. Anal. Calcd for $C_{42}H_{34}F_{12}N_{10}P_2Os{\cdot}H_2O$: C, 42.86; H, 3.08; N, 11.90. Found: C, 42.98; H, 3.40; N, 11.80.

Synthesis of Complex [Os(Mebip)(tpy)](PF$_6$)$_2$, 6(PF$_6$)$_2$. Using the same procedure for the synthesis of $\mathbf{1}(PF_6)_2$, 15.8 mg of $\mathbf{6}(PF_6)_2$ was obtained from the reaction of $[(Mebip)OsCl_3]$ (31.8 mg, 0.050 mmol) and tpy (20.1 mg, 0.080 mmol) in 30% yield. ^{1}H NMR (400 MHz, CD_3CN): δ 4.52 (s, 6H), 5.94 (d, J = 8.4 Hz, 2H), 6.93 (m, 2H), 7.02 (m, 2H), 7.25 (d, J = 5.6 Hz, 2H), 7.38 (m, 2H), 7.54 (d, J = 8.4 Hz, 2H), 7.61 (m, 2H), 7.76 (t, J = 8.4 Hz, 1H), 7.97 (t, J = 8.2 Hz, 1H), 8.35 (d, J = 8.0 Hz, 2H), 8.70 (d, J = 8.4 Hz, 2H), 8.82 (d, J = 8.4 Hz, 2H). MALDI-MS: 908.5 for $[M - PF_6]^+$, 762.4 for $[M - 2PF_6]^+$. Anal. Calcd for $C_{36}H_{28}F_{12}N_8P_2Os{\cdot}H_2O$: C, 40.38; H, 2.82; N, 10.46. Found: C, 39.98; H, 2.91; N, 10.83.

Electrochemical Measurements. All CV measurements were taken using a CHI620D potentiostat with a one-compartment electrochemical cell under an atmosphere of nitrogen. All measurements were carried out in denoted solvents containing 0.1 M ^{n}Bu$_4$NClO$_4$ as the supporting electrolyte at a scan rate of 100 mV/s. The working electrode was a glassy carbon with a diameter of 3 mm. The electrode was polished prior to use with 0.05 μm alumina and rinsed thoroughly with water and acetone. A large area platinum wire coil was used as the counter electrode. All potentials are referenced to the Ag/AgCl electrode in saturated aqueous NaCl without regard for the liquid junction potential. Potentials vs ferrocene$^{0/+}$ can be deduced by subtracting 0.45 V.

Spectroscopic Measurements. UV–vis and NIR spectra were recorded on a TU-1810DSPC or a PE Lambda 750 UV/vis/NIR spectrophotometer at room temperature in CH_3CN, with a conventional 1 cm quartz cell. Emission spectra were recorded using an F-380 spectrofluorimeter of Tianjin Gangdong Sic. & Tech Development Co. Ltd., with a red-sensitive photomultiplier tube R928F. Spectroelectrochemistry was performed in a thin layer cell (optical length = 0.1 cm) in which an ITO glass working electrode was set. A platinum wire and Ag/AgCl in saturated aqueous NaCl was used as a counter electrode and a reference electrode, respectively. The cell was put into the spectrometer to monitor the spectral change during electrolysis.

X-ray Crystallography. The X-ray diffraction data were collected using a Rigaku Saturn 724 diffractometer on a rotating anode (Mo–K radiation, 0.71073 Å) at 173 K. The structure was solved by the direct method using SHELXS-97[21] and refined with Olex2.[22] The structure graphics shown in shown in Figure 1 were generated using Olex2. The corresponding CIF files are provided in the Supporting Information.

Computational Methods. All calculations were implemented in the Gaussian 09 program.[23] Wave functions were expanded in the LANL2DZ basis set with effective core potentials,[24] and electron exchange-correlation was described using the B3LYP hybrid functional.[25] No symmetry constraints were used in the optimization (nosymm keyword was used). Solvation effects in CH_3CN were included using the conductor-like polarizable continuum model (CPCM) with united-atom Kohn–Sham (UAKS) radii.[26] Frequency calculations have been performed with the same level of theory to ensure the optimized geometries to be local minima. All orbitals have been computed at an isovalue of 0.03 e/bohr^3. The TDDFT-predicted spectra were generated using GaussView 5.0.

■ ASSOCIATED CONTENT

Ⓢ Supporting Information

X-ray crystallographic data for $\mathbf{2}(PF_6)$ and $\mathbf{6}(PF_6)_2$ in CIF format, isodensity plots of frontiers orbitals, TDDFT results, Cartesian coordinates for DFT-optimized structures, and NMR and mass spectra of new complexes. This material is available free of charge via the Internet at http://pubs.acs.org.

■ AUTHOR INFORMATION

Corresponding Author

*E-mail: zhongyuwu@iccas.ac.cn.

Notes

The authors declare no competing financial interest.

■ ACKNOWLEDGMENTS

This work is supported by the National Natural Science Foundation of China (grants 21002104, 91227104, 21271176, and 212210017), the National Basic Research 973 program of China (grant 2011CB932301), and the Institute of Chemistry, Chinese Academy of Sciences ("100 Talent" Program and grant CMS-PY-201230) for funding support.

■ REFERENCES

(1) (a) Schubert, U. S.; Eschbaumer, C. *Angew. Chem., Int. Ed.* **2002**, *41*, 2892. (b) Eryazici, I.; Moorefield, C. N.; Newkome, G. R. *Chem. Rev.* **2008**, *108*, 1834. (c) Medlycott, E. A.; Hanan, G. S. *Chem. Soc. Rev.* **2005**, *34*, 133. (d) Williams, J. A. G. *Chem. Soc. Rev.* **2009**, *38*, 1783.

(2) (a) Bruce, M. I. *Angew. Chem., Int. Ed.* **1977**, *16*, 73. (b) van der Boom, M. E.; Milstein, D. *Chem. Rev.* **2003**, *103*, 1759. (c) Chi, Y.; Chou, P.-T. *Chem. Soc. Rev.* **2010**, *39*, 638. (d) Albrecht, M. *Chem. Rev.* **2010**, *110*, 576.

(3) (a) Djukic, J.-P.; Sortais, J.-B.; Barloy, L.; Pfeffer, M. *Eur. J. Inorg. Chem.* **2009**, 817. (b) Reveco, P.; Cherry, W. R.; Medley, J.; Garber, A.; Gale, R. J.; Selbin, J. *Inorg. Chem.* **1986**, *25*, 1842. (c) Coudret, C.; Fraysse, S.; Launay, J.-P. *Chem. Commun.* **1998**, 663. (d) Duprez, V.; Launay, J.-P.; Gourdon, A. *Inorg. Chim. Acta* **2003**, *343*, 395. (e) Moorlag, C.; Wolf, M. O.; Bohne, C.; Patrick, B. O. *J. Am. Chem. Soc.* **2005**, *127*, 6382. (f) Wadman, S. H.; Lutz, M.; Tooke, D. M.; Spek, A. L.; Hartl, F.; Havenith, R. W. A.; van Klink, G. P. M.; van Koten, G. *Inorg. Chem.* **2009**, *48*, 1887. (g) Jäger, M.; Smeigh, A.; Lombeck, F.; Görls, H.; Collin, J.-P.; Sauvage, J.-P.; Hammarström, L.; Johannsson, O. *Inorg. Chem.* **2010**, *49*, 374. (h) Zhong, Y.-W.; Wu, S.-H.; Burkhardt, S. E.; Yao, C.-J.; Abruña, H. D. *Inorg. Chem.* **2011**, *50*, 517. (i) Yang, W.-W.; Wang, L.; Zhong, Y.-W.; Yao, J. *Organometallics* **2011**, *30*, 2236. (j) Wu, S.-H.; Burkhardt, S. E.; Zhong, Y.-W.; Abruña, H. D. *Inorg. Chem.* **2012**, *51*, 13312. (k) Schulze, B.; Escudero, D.; Friebe, C.; Siebert, R.; Gorls, H.; Sinn, S.; Thomas, M.; Mai, S.; Popp, J.; Dietzek, B.; Gonzalez, L.; Schubert, U. S. *Chem.—Eur. J.* **2012**, *18*, 4010. (l) Padhi, S. K.; Tanaka, K. *Inorg. Chem.* **2011**, *50*, 10718.

(4) (a) You, Y.; Park, S. Y. *Dalton Trans.* **2009**, 1267. (b) Chen, Z.-q.; Bian, Z.-q.; Huang, C.-h. *Adv. Mater.* **2010**, *22*, 1534. (c) Polson, M.; Ravaglia, Fracasso, S.; Garavelli, M.; Scandola, F. *Inorg. Chem.* **2005**, *44*, 1282. (d) Wilkinson, A. J.; Goeta, A. E.; Foster, C.; Williams, J. A. G. *Inorg. Chem.* **2004**, *43*, 6513.

(5) (a) Lu, W.; Mi, B.-X.; Chan, M. C. W.; Hui, Z.; Che, C.-M.; Zhu, N.; Lee, S.-T. *J. Am. Chem. Soc.* **2004**, *126*, 4958. (b) Shao, P.; Li, Y.; Yi, J.; Pritchett, T. M.; Sun, W. *Inorg. Chem.* **2010**, *49*, 4507. (c) Hofmann, A.; Dahlenburg, L.; van Eldik, R. *Inorg. Chem.* **2003**, *42*, 6528. (d) Cheung, T.-C.; Cheung, K.-K.; Peng, S.-M.; Che, C.-M. *J. Chem. Soc., Dalton Trans.* **1996**, 1645. (e) Wu, S.-H.; Burkhardt, S. E.; Yao, J.; Zhong, Y.-W.; Abruña, H. D. *Inorg. Chem.* **2011**, *50*, 3959.

(6) (a) Costa, R. D.; Orti, E.; Bolink, H. J.; Monti, F.; Accorsi, G.; Armaroli, N. *Angew. Chem., Int. Ed.* **2012**, *51*, 8178. (b) Evans, R. C.; Douglas, P.; Winscom, C. J. *Coord. Chem. Rev.* **2006**, *250*, 2093. (c) Lowry, M. S.; Bernhard, S. *Chem.—Eur. J.* **2006**, *12*, 7970. (d) Wong, W.-Y.; Ho, C.-L. *J. Mater. Chem.* **2009**, *19*, 4457.

(7) (a) Wadman, S. H.; Kroom, J. M.; Bakker, K.; Lutz, M.; Spek, A. L.; van Klink, G. P. M.; van Koten, G. *Chem. Commun.* **2007**, 1907. (b) Bessho, T.; Yoneda, E.; Yum, J.-H.; Guglielmi, M.; Tavernelli, I.; Imai, H.; Rothlisberger, U.; Nazeeruddin, M. K.; Gratzel, M. *J. Am. Chem. Soc.* **2009**, *131*, 5930. (c) Bomben, P. G.; Koivisto, B. D.; Berlinguette, C. P. *Inorg. Chem.* **2010**, *49*, 4960. (d) Wadman, S. H.; Kroon, J. M.; Bakker, K.; Havenith, R. W. A.; van Klink, G. P. M.; van Koten, G. *Organometallics* **2010**, *29*, 1569. (e) Robson, K. C. D.; Koivisto, B. D.; Yella, A.; Sporinova, B.; Nazeeruddin, M. K.; Baumgartner, T.; Gratzel, M.; Berlinguette, C. P. *Inorg. Chem.* **2011**, *50*, 5494. (f) Bomben, P. G.; Gordon, T. J.; Schott, E.; Berlinguette, C. P. *Angew. Chem., Int. Ed.* **2011**, *50*, 10682. (g) Bomben, P. G.; Robson, K. C. D.; Koivisto, B. D.; Berlinguette, C. P. *Coord. Chem. Rev.* **2012**, *256*, 1438.

(8) (a) Beley, M.; Collin, J.-P.; Louis, R.; Metz, B.; Sauvage, J.-P. *J. Am. Chem. Soc.* **1991**, *113*, 8521. (b) Sutter, J.-P.; Grove, D. M.; Beley, M.; Collin, J.-P.; Veldman, N.; Spek, A. L.; Sauvage, J.-P.; van Koten, G. *Angew. Chem., Int. Ed.* **1994**, *33*, 1282. (c) Patoux, C.; Launay, J.-P.; Beley, M.; Chodorowski-Kimmers, S.; Collin, J.-P.; James, S.; Sauvage, J.-P. *J. Am. Chem. Soc.* **1998**, *120*, 3717. (d) Steenwinkel, P.; Grove, D. M.; Veldman, N.; Spek, A. L.; van Koten, G. *Organometallics* **1998**, *17*, 5647. (e) Fraysse, S.; Coudret, C.; Launay, J.-P. *J. Am. Chem. Soc.* **2003**, *125*, 5880. (f) Gagliardo, M.; Amijs, C. H. M.; Lutz, M.; Spek, A. L.; Havenith, R. W. A.; Hartl, F.; van Klink, G. P. M.; van Koten, G. *Inorg. Chem.* **2007**, *46*, 11133. (g) Yang, W.-W.; Yao, J.; Zhong, Y.-W. *Organometallics* **2012**, *31*, 1035. (h) Yao, C.-J.; Zhong, Y.-W.; Yao, J. *J. Am. Chem. Soc.* **2011**, *133*, 15697. (i) Yao, C.-J.; Sui, L.-Z.; Xie, H.-Y.; Xiao, W.-J.; Zhong, Y.-W.; Yao, J. *Inorg. Chem.* **2010**, *49*, 8347.

(9) (a) Mortimer, R. J. *Chem. Soc. Rev.* **1997**, *26*, 147. (b) Ward, M. D. *J. Solid State Electrochem.* **2005**, *9*, 778. (c) Yao, C.-J.; Zhong, Y.-W.; Nie, H.-J.; Abruña, H. D.; Yao, J. *J. Am. Chem. Soc.* **2011**, *133*, 20720. (d) Yao, C.-J.; Yao, J.; Zhong, Y.-W. *Inorg. Chem.* **2012**, *51*, 6259.

(10) (a) Yang, W.-W.; Zhong, Y.-W.; Yoshikawa, S.; Shao, J.-Y.; Masaoka, S.; Sakai, K.; Yao, J.; Haga, M.-a. *Inorg. Chem.* **2012**, *51*, 890. (b) Shao, J.-Y.; Yang, W.-W.; Yao, J.; Zhong, Y.-W. *Inorg. Chem.* **2012**, *51*, 4343. (c) Shao, J.-Y.; Yao, J.; Zhong, Y.-W. *Organometallics* **2012**, *31*, 4302.

(11) (a) Kober, E. M.; Caspar, J. V.; Sullivan, B. P.; Meyer, T. J. *Inorg. Chem.* **1988**, *27*, 4587. (b) Zhong, Y.-W.; Vila, N.; Henderson, J. C.; Flores-Torres, S.; Abruña, H. D. *Inorg. Chem.* **2007**, *46*, 10470. (c) Srnec, M.; Chalupsky, J.; Fojta, M.; Zendlova, L.; Havran, L.; Hocek, M.; Kyvala, M.; Rulisek, L. *J. Am. Chem. Soc.* **2008**, *130*, 10947.

(12) (a) Jameson, G. B.; Muster, A.; Robinson, S. D.; Wingfield, J. N.; Ibers, J. A. *Inorg. Chem.* **1981**, *20*, 2448. (b) Wen, T. B.; Cheung, Y. K.; Yao, J.; Wong, W.-T.; Zhou, Z. Y.; Jia, G. *Organometallics* **2000**, *19*, 3803. (c) Gusev, D. G.; Dolgushin, F. M.; Antipin, M. Y. *Organometallics* **2001**, *20*, 1001. (d) Majumder, K.; Peng, S.-M.; Bhattacharya, S. *J. Chem. Soc., Dalton Trans.* **2001**, 284. (e) Hwang, K.-C.; Chen, J.-L.; Chi, Y.; Lin, C.-W.; Cheng, Y.-M.; Lee, G.-H.; Chou, P.-T.; Lin, S.-Y.; Shu, C.-F. *Inorg. Chem.* **2008**, *47*, 3307.

(13) (a) Ryabov, A. D.; Soukharev, V. S.; Alexandrova, L.; Le Lagadec, R.; Pfeffer, M. *Inorg. Chem.* **2003**, *42*, 6598. (b) Ceron-Camacho, R.; Morales-Morales, D.; Hernandez, S.; Le Lagadec, R.; Ryabov, A. D. *Inorg. Chem.* **2008**, *47*, 4988. (c) Ceron-Camacho, R.; Hernanzez, S.; Le Legadec, R. *Chem. Commun.* **2011**, *47*, 2823.

(14) (a) Beley, M.; Collin, J.-P.; Sauvage, J.-P. *Inorg. Chem.* **1993**, *32*, 4539. (b) Beley, M.; Chodorowski, S.; Collin, J.-P.; Sauvage, J.-P.; Flamigni, L.; Barigelletti, F. *Inorg. Chem.* **1994**, *33*, 2543.

(15) Chung, L.-H.; Chan, S.-C.; Lee, W.-C.; Wong, C.-Y. *Inorg. Chem.* **2012**, *51*, 8693.

(16) (a) Haga, M.; Takasugi, T.; Tomie, A.; Ishizuya, M.; Yamada, T.; Hossain, M. D.; Inoue, M. *Dalton Trans.* **2003**, 2069. (b) Terada, K.; Kobayashi, K.; Haga, M. *Dalton Trans.* **2008**, 4846. (c) Haga, M.; Hong, H.-G.; Shiozawa, Y.; Kawata, Y.; Monjushiro, H.; Fukuo, T.; Arakawa, R. *Inorg. Chem.* **2000**, *39*, 4566. (d) Yutaka, T.; Obara, S.; Ogawa, S.; Nozaki, K.; Ikeda, N.; Ohno, T.; Ishii, Y.; Sakai, K.; Haga, M. *Inorg. Chem.* **2005**, *44*, 4737. (e) Obara, S.; Itabashi, M.; Okuda, F.; Tamaki, S.; Tanabe, Y.; Ishii, Y.; Nozaki, K.; Haga, M. *Inorg. Chem.* **2006**, *45*, 8907. (f) Ruttimann, S.; Bernardinelli, G.; Williams, A. F. *Angew. Chem., Int. Ed.* **1993**, *32*, 392. (g) Carina, R. F.; Williams, A. F.; Bernardinelli, G. *Inorg. Chem.* **2001**, *40*, 1826. (h) Tam, A. Y.-Y.; Lam, W. H.; Wong, K. M.-C.; Zhu, N.; Yam, V. W.-W. *Chem.—Eur. J.* **2008**, *14*, 4562. (i) Mathew, I.; Sun, W. *Dalton Trans.* **2010**, *39*, 5885. (j) Wang, K.; Haga, M.; Monjushiro, H.; Akiba, M.; Sasaki, Y. *Inorg. Chem.* **2000**, *39*, 4022. (k) Terazzi, E.; Guenee, L.; Morgantini, P.-Y.; Bernardinelli, G.; Donnio, B.; Guillon, D.; Piguet, C. *Chem.—Eur. J.* **2007**, *13*, 1674. (l) Tam, A. Y.-Y.; Tsang, D. P.-K.; Chan, M.-Y.; Zhu, N.; Yam, V. W.-W. *Chem. Commun.* **2011**, *47*, 3383.

(17) We use ttpy as a substitute for tpy, because ttpy is much easier to be synthesized and they have similar electronic properties. Wang, J.; Hanan, G. S. *Synlett* **2005**, 1251.

(18) (a) Collin, J.-P.; Guillerez, S.; Sauvage, J.-P. *J. Chem. Soc., Chem. Commun.* **1989**, 776. (b) Akasaka, T.; Mutai, T.; Otsuki, J.; Araki, K. *Dalton Trans.* **2003**, 1537.
(19) (a) Yao, C.-J.; Zheng, R.-H.; Shi, Q.; Zhong, Y.-W.; Yao, J. *Chem. Commun.* **2012**, *48*, 5680. (b) Connelly, N. G.; Geiger, W. E. *Chem. Rev.* **1996**, *96*, 877.
(20) Wang, Z.; Turner, E.; Mahoney, V.; Madakuni, S.; Groy, T.; Li, J. *Inorg. Chem.* **2010**, *49*, 11276.
(21) Sheldrick, G. M. *Acta Crystallogr.* **2008**, *A64*, 112.
(22) Dolomanov, O. V.; Bourhis, L. J.; Gildea, R. J.; Howard, J. A. K.; Puschmann, H. *J. Appl. Crystallogr.* **2009**, *42*, 339.
(23) Frisch, M. J.; Trucks, G. W.; Schlegel, H. B.; Scuseria, G. E.; Robb, M. A.; Cheeseman, J. R.; Montgomery, J. A.; Vreven, T., Jr.; Kudin, K. N.; Burant, J. C.; Millam, J. M.; Iyengar, S. S.; Tomasi, J.; Barone, V.; Mennucci, B.; Cossi, M.; Scalmani, G.; Rega, N.; Petersson, G. A.; Nakatsuji, H.; Hada, M.; Ehara, M.; Toyota, K.; Fukuda, R.; Hasegawa, J.; Ishida, M.; Nakajima, T.; Honda, Y.; Kitao, O.; Nakai, H.; Klene, M.; Li, X.; Knox, J. E.; Hratchian, H. P.; Cross, J. B.; Adamo, C.; Jaramillo, J.; Gomperts, R.; Stratmann, R. E.; Yazyev, O.; Austin, A. J.; Cammi, R.; Pomelli, C.; Ochterski, J. W.; Ayala, P. Y.; Morokuma, K.; Voth, G. A.; Salvador, P.; Dannenberg, J. J.; Zakrzewski, V. G.; Dapprich, S.; Daniels, A. D.; Strain, M. C.; Farkas, O.; Malick, D. K.; Rabuck, A. D.; Raghavachari, K.; Foresman, J. B.; Ortiz, J. V.; Cui, Q.; Baboul, A. G.; Clifford, S.; Cioslowski, J.; Stefanov, B. B.; Liu, G.; Liashenko, A.; Piskorz, P.; Komaromi, I.; Martin, R. L.; Fox, D. J.; Keith, T.; Al-Laham, M. A.; Peng, C. Y.; Nanayakkara, A.; Challacombe, M.; Gill, P. M. W.; Johnson, B.; Chen, W.; Wong, M. W.; Gonzalez, C.; Pople, J. A. *Gaussian 09*, revision A.2; Gaussian, Inc.: Wallingford, CT, 2009.
(24) (a) Dunning, T. H.; Hay, P. J. In *Modern Theoretical Chemistry*; Schaefer, H. F., Ed.; Plenum: New York, 1976; Vol. 3, p 1. (b) Hay, P. J.; Wadt, W. R. *J. Chem. Phys.* **1985**, *82*, 270. (c) Wadt, W. R.; Hay, P. J. *J. Chem. Phys.* **1985**, *82*, 284. (d) Hay, P. J.; Wadt, W. R. *J. Chem. Phys.* **1985**, *82*, 299.
(25) (a) Becke, A. D. *J. Chem. Phys.* **1993**, *98*, 5648. (b) Lee, C.; Yang, W.; Parr, R. G. *Phys. Rev. B* **1988**, *37*, 785.
(26) (a) Klamt, A.; Schüürmann, G. *J. Chem. Soc., Perkin Trans. 2* **1993**, 799. (b) Andzelm, J.; Kölmel, C.; Klamt, A. *J. Chem. Phys.* **1995**, *103*, 9312. (c) Barone, V.; Cossi, M. *J. Phys. Chem. A* **1998**, *102*, 1995. (d) Cossi, M.; Rega, N.; Scalmani, G.; Barone, V. *J. Comput. Chem.* **2003**, *24*, 669. (e) Takano, Y.; Houk, K. N. *J. Chem. Theory Comput.* **2005**, *1*, 70.